

STABILIZATION OF THE CLASSICAL SHIMMYING WHEEL

Bill Goodwine

Division of Engineering and Applied Science
California Institute of Technology
Pasadena, California 91106
Fax: (818) 568-2719
E-mail: goodwine@robby.caltech.edu

Gábor Stépán

Department of Applied Mechanics
Technical University of Budapest
H-1521 Budapest, Hungary
Fax: (361) 463-3470
E-mail: stepan@mm.bme.edu

ABSTRACT

Many vehicle systems contain rolling elements which exhibit unstable rolling motion, called shimmying, which may lead to disastrous results. The *classical shimmying wheel* is a simple model which captures the essential dynamics of such systems. Fortunately, this model possesses a particular geometric structure which provides a simple means to design a globally stabilizing controller. However, this model is limited because it assumes that the wheel rolls without slipping, and for real systems, the wheel may slip because the constraint force, applied by friction, is bounded. The controller which globally stabilizes the rolling system sometimes fails to stabilize the slipping system. An alternative control strategy is proposed which is more effective in stabilizing the slipping system.

INTRODUCTION

Unstable rolling is an important phenomenon in vehicle dynamics, affecting many systems such as aircraft nose wheels, truck trailers and motorcycle wheels. One particular model, which we call the *classical shimmying wheel*, is the focus of this paper. Although the dynamics of this system are rich and complex, the model is *feedback linearizable*, so there exists a nonlinear coordinate transformation through which the control system is transformed into a system which is linear and controllable. We design a controller using this method and verify its efficacy via numerical simulations.

We also consider the more realistic model where the wheel is allowed to slip if the rolling constraint force exceeds that which can be supplied by friction. This more realistic system evolves in either a four or six-dimensional phase space, corresponding to pure rolling and slipping, respectively, and may alternate between them. Given the strongly nonlinear nature of this system, it is not surprising that it can exhibit chaotic behavior. When used on this more complex model, the controller designed for the purely rolling system sometimes fails to stabilize the system. Numerical simulations suggest that an alternative control strategy in which the controller is only utilized

while the system is purely rolling is an extremely effective stabilizing control strategy. This alternative approach is appealing because it directly utilizes the existence of a chaotic attractor present in the slipping system.

A schematic drawing of the classical shimmying wheel model is shown in Figure 1. We consider the kingpin assembly which connects the body to the rod to be massless and the control input to be a torque, u , about the kingpin. Also, we consider the body to be moving with a constant velocity v . The configuration variables are the kingpin displacement y , the bar angle θ , and the wheel rotation angle ϕ .

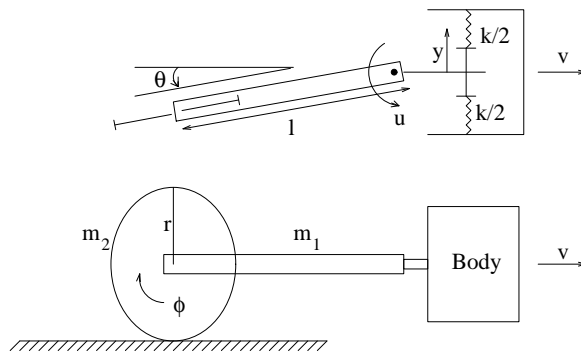


Fig. 1. Wheel Model

UNCONTROLLED DYNAMICS

The equations of motion for the purely rolling system with ideal nonholonomic constraints and control input u are

$$\begin{aligned} \ddot{\theta} &= \frac{-\frac{v}{l} \left(\sec^2 \theta - \frac{1}{2} + \frac{3m_2}{2m_1} \tan^2 \theta \right) \dot{\theta}}{\left(\frac{1}{3} + \tan^2 \theta \right) \cos \theta + \frac{m_2}{4m_1} \left(\frac{r^2}{l^2} \cos \theta + 6 \tan^2 \theta \cos \theta \right)} \\ &\quad - \frac{\frac{k}{lm_1} y + \left(1 + \frac{3m_2}{2m_1} \right) \frac{\tan \theta}{\cos \theta} \dot{\theta}^2 - \frac{\cos \theta}{l^2 m_1} u}{\left(\frac{1}{3} + \tan^2 \theta \right) \cos \theta + \frac{m_2}{4m_1} \left(\frac{r^2}{l^2} \cos \theta + 6 \tan^2 \theta \cos \theta \right)} \\ \dot{y} &= l \dot{\theta} \cos \theta + \left(v + l \dot{\theta} \sin \theta \right) \tan \theta \\ \dot{\phi} &= \frac{\sec \theta \left(v + l \dot{\theta} \sin \theta \right)}{r}. \end{aligned}$$

A complete study of the dynamics of this system is presented in (Stépán, 1991), where it was shown that if $3m_2 r^2 < 2m_1 l^2$, then the system was linearly stable

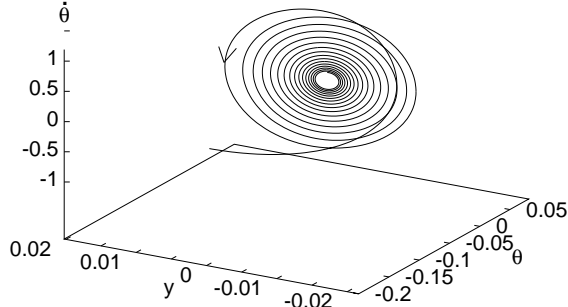


Fig. 2. Locally Stable Rolling System

about the $\theta = 0$ and $y = 0$ position, and linearly unstable otherwise. Additionally, it was shown by the Hopf bifurcation method, that an unstable limit cycle exists around the asymptotically stable stationary motion.

If we set $u = 0$, we can numerically verify the above results. For $m_1 = 1.5$, $m_2 = 2.75$, $l = 0.2$, $r = 0.1$, $k = 75$ and $v = 1$, given in SI units, Figure 2 shows the stability of the equilibrium solution. If $m_2 = 4.75$, Figure 3 shows the saddle nature of the instability of the equilibrium solution with θ approaching $\pm\pi/2$. Figure 4 shows two solutions, a stable solution with initial conditions inside the unstable limit cycle and an unstable solution with initial conditions outside the unstable limit cycle. For the stable solution, the initial conditions are $\theta_0 = -0.24$ and $\dot{\theta}_0 = 0.4$, and for the unstable solution, $\theta_0 = -0.24$ and $\dot{\theta}_0 = 0.0$. In this simulation, all the parameters are the same as before, except $m_2 = 3.75$ (which satisfies the local stability condition).

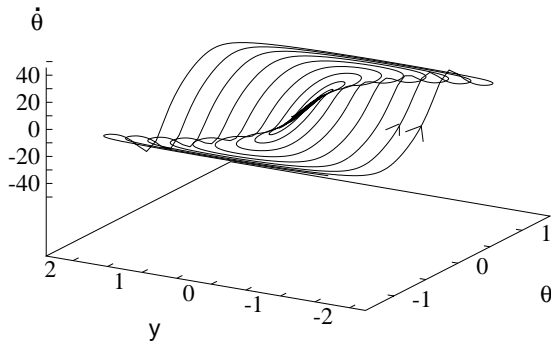


Fig. 3. Locally Unstable Rolling System

Now we assume that the dynamics of the system switch from a pure rolling condition to a slipping condition if the magnitude of the constraining force exceeds that which can be applied by friction. We assume that the dynamics of the system switch back from slipping to pure rolling when the velocity of the point of contact between the wheel and surface is zero and the constraint force does not exceed the maximum friction force.

The equations of motion for the slipping system

are

$$\begin{pmatrix} (\frac{1}{3}m_1 + (1 + \frac{r^2}{4l^2})m_2)l^2 & -Ml \cos \theta & 0 \\ -Ml \cos \theta & m_1 + m_2 & 0 \\ 0 & 0 & \frac{1}{2}m_2 r^2 \end{pmatrix} \begin{pmatrix} \ddot{\theta} \\ \ddot{y} \\ \dot{\phi} \end{pmatrix} = \begin{pmatrix} \frac{v_{px}}{\sqrt{v_{px}^2 + v_{py}^2}} M l \mu_d g + u \\ -M l \dot{\theta}^2 \sin \theta - k y - \frac{v_{px} \sin \theta + v_{py} \cos \theta}{\sqrt{v_{px}^2 + v_{py}^2}} M \mu_d g \\ \frac{v_{px}}{\sqrt{v_{px}^2 + v_{py}^2}} M r \mu_d g \end{pmatrix},$$

where v_{px} and v_{py} represent the two components of the velocity of the point of contact of the wheel with the surface, μ_d is the slipping (dynamic) coefficient of friction and $M = \frac{1}{2}m_1 + m_2$.

In the following simulations, the constraint force is evaluated using Lagrange multipliers. This may lead to results which are slightly different than in (Stépán, 1991), which used an approximation to determine when to switch from rolling to slipping.

Figure 5 shows an enlarged view of a portion of the response of the system with a coefficient of static (pure rolling) friction, $\mu_s = 0.2$ and a coefficient of dynamic (slipping) friction of $\mu_d = 0.1$. All other parameters are the same as before, except $m_2 = 3.75$. This illustrates one aspect of the chaotic behavior discussed in (Stépán, 1991).

FEEDBACK LINEARIZATION

Consider the control system described by

$$\Sigma_0 = \begin{cases} \dot{x} &= f(x) + g(x)u \\ y &= h(x), \end{cases}$$

where h is called the *output function* and $\dim(x) = n$. This system has *relative degree* r at a point x_0 if

1. $L_g L_f^k h(x) = 0 \forall x$ in a neighborhood of x_0 , and all $k < r - 1$, and
2. $L_g L_f^{r-1} h(x_0) \neq 0$,

where $L_g h$ is the Lie derivative of the function h along the vector field g .

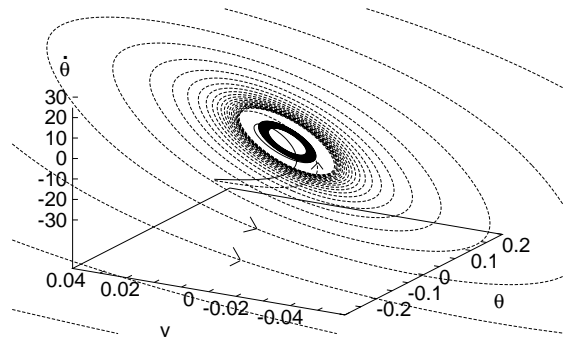


Fig. 4. Unstable Limit Cycle

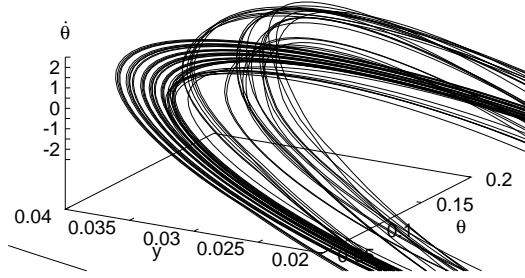


Fig. 5. Chaotic Behavior

If $r = n$ for all x , consider the change of coordinates

$$\begin{aligned}\xi_1 &= h(x) \\ \xi_2 &= \dot{\xi}_1 = L_f h(x) \\ \xi_3 &= \dot{\xi}_2 = L_f^2 h(x) \\ &\vdots \\ \xi_n &= \dot{\xi}_{n-1} = L_f^{n-1} h(x) \\ &\quad \dot{\xi}_n = L_f^n h(x) + L_g L_f^{n-1} h(x) u.\end{aligned}$$

Since $L_g L_f^{n-1} h(x) \neq 0 \forall x$, we can define

$$u = \frac{1}{L_g L_f^{n-1} h(x)} (-L_f^n h(x) + v)$$

so that $\dot{\xi}_n = v$. In this manner, the nonlinear control system Σ_0 is transformed into a controllable linear system. If $h_d(t)$ is the desired “trajectory,” choose

$$v = \dot{h}_d^{(n)} + \alpha_{n-1}(h_d^{(n-1)} - \xi_n) + \dots + \alpha_0(h_d - \xi_1),$$

as a feedback control law where the α_i are such that $s^n + \alpha_{n-1}s^{n-1} + \dots + \alpha_1s + \alpha_0$ is a Hurwitz polynomial. For a complete explanation see (Isidori, 1989), and (Nijmeijer and van der Schaft, 1990).

For an arbitrary system, there is no general method for constructing an output function, h , which generates the coordinate transformation under which the system is rendered linear. In the case of the classical shimmying wheel (the purely rolling case) the ϕ -coordinate is cyclic, so we can consider $x = (\theta, y, \theta)$ and write the system as $f(x) + g(x)u$, where $g(x)$ is simply the terms in $\dot{\theta}$ which contain the control input term, u , and $f(x)$ contains all the other terms in the equations of motion.

If we consider $h_1 = y$ as a candidate output function,

$$\begin{aligned}L_g h_1 &= 0 \\ L_f h_1 &= l\dot{\theta} \cos \theta + (v + l\dot{\theta} \sin \theta) \tan \theta \\ L_g L_f h &\neq 0.\end{aligned}$$

Since $L_g L_f h \neq 0$, h_1 is not an output function which renders the system feedback linearizable. Note, however, that if another output function, h_2 were purely

a function of θ , then

$$L_f h_2 = \frac{dh_2}{d\theta} \dot{\theta},$$

since the θ component of f is simply $\dot{\theta}$. Since $L_f h_1$ is linear in $\dot{\theta}$, and otherwise only a function of θ , we can differentiate it with respect to $\dot{\theta}$, integrate it with respect to θ , and subtract h_1 from the result. If we denote the resulting function by h , we have

$$h(x) = -y - l \log\left(\cos \frac{\theta}{2} - \sin \frac{\theta}{2}\right) + l \log\left(\cos \frac{\theta}{2} + \sin \frac{\theta}{2}\right),$$

where h renders the system feedback linearizable via the preceding construction.

SIMULATION RESULTS

The results of a simulation which illustrates that the controller stabilizes the system when the physical parameters do not satisfy the linear stability criterion are presented in Figure 6. In this simulation, $m_2 = 5.75$ and the initial conditions are $(\theta, y, \phi, \dot{\theta}) = (-0.75, 0, 0, 0)$.

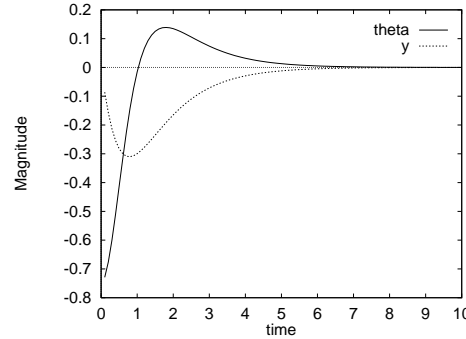


Fig. 6. Controlled Pure Rolling System

To attempt to stabilize the slipping system, the obvious first attempt would be to use the same controller on the slipping system. Figure 7 show the results of a simulation where the controller stabilizes the slipping system. In this simulation, we take the physical parameters to be the same as before, except $m_2 = 5.75$, which makes the equilibrium solution locally unstable, and $\mu_s = 0.4$ and $\mu_d = 0.2$. We take the initial conditions to be $(\theta, y, \phi, \dot{\theta}, \dot{\phi}) = (-0.5, 0, 0, 0, 0)$.

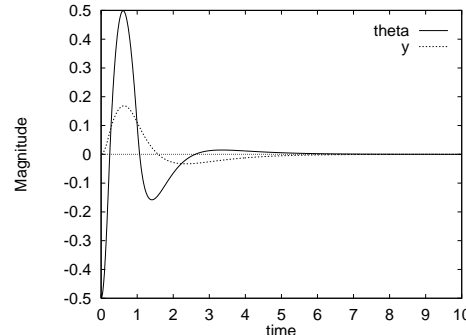


Fig. 7. Controlled Slipping System

Note, however, for the same initial conditions, but for $\mu_s = 0.2$ and $\mu_d = 0.1$, the controller fails to stabilize the system. See Figure 8.

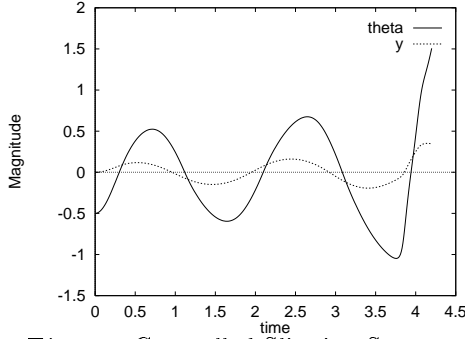


Fig. 8. Controlled Slipping System

These, and other numerical experiments indicate that the controller is stabilizing for a region of the phase space that gets larger as the coefficient of friction increases. This makes intuitive sense because as the coefficient of friction increases, the system is, in some sense, “closer” to the system for which the controller was designed.

AN ALTERNATIVE APPROACH

If we adopt a slightly different approach, however, better results are obtained. If the initial conditions for the system are in the slipping regime and the parameter values for the system are such that a chaotic attractor exists, the solution will approach the chaotic attractor. If we set the control input to zero until the solution is near this attractor, indicated by a switch from slipping to rolling, better results are obtained. Specifically, we choose the control strategy where the control input is zero if the wheel is slipping, and the controller designed previously is utilized if the wheel is rolling. Figure 9 shows simulation results for the system with the same physical parameters and initial conditions as the preceding simulation.

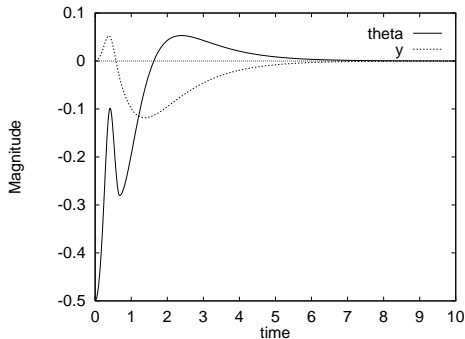


Fig. 9. Alternative Control Strategy

At least with regard to numerical experimentation, this control strategy seems globally stabilizing with respect to initial conditions in θ as well as variations in μ_s , μ_d , m_1 and m_2 . Figure 10 shows the results when the initial conditions are $(\theta, y, \phi, \dot{\theta}, \dot{y}, \dot{\phi}) = (-3.0, 0, 0, 0, 0, 0)$. Extensive numerical experimentation suggests that this strategy is very effective. The only apparent problem is that the strategy does not always stabilize the system when $\mu_s = \mu_d$, which, fortunately, is a physically unrealistic situation.

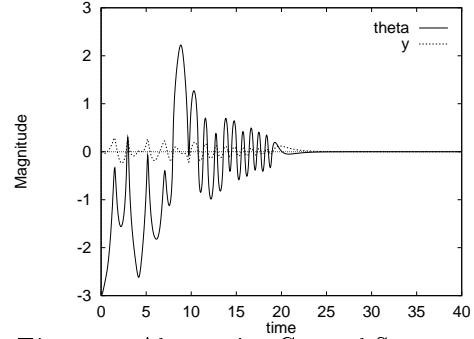


Fig. 10. Alternative Control Strategy

CONCLUSIONS

In this paper, we have presented and illustrated a particular controller design for the classical shimmying wheel. The controller is guaranteed to be globally stabilizing for the wheel when it rolls without slipping, but sometimes fails to stabilize the system when the wheel is allowed to slip. However, based upon numerical simulations, the alternative control strategy seems effective in stabilizing the slipping system.

Of course, there are many more avenues available for investigation. Obviously, more work is required to determine the nature of the chaotic attractor and its relationship to the purely rolling regimes where the controller is guaranteed to stabilize the system. Another avenue of study would be to study the efficacy of the controller designed here on a more realistic model of an elastic tire. Also, investigating the geometric nature of a more realistic tire model, such as presented in (Barta and Stépán, 1995) may yield insights into controller design for practical implementation.

References

- Barta, G. and Stépán, G. (1995). Untersuchung quasi-periodischer schwingungen von mit reifen versehenen radern. *ZAMM*, 75:S77–S78.
- Isidori, A. (1989). *Nonlinear Control Systems*. Springer–Verlag, second edition.
- Nijmeijer, H. and van der Schaft, A. J. (1990). *Nonlinear Dynamical Control Systems*. Springer–Verlag.
- Nimark, J. I. and Fufaiv, N. A. (1972). *Dynamics of Nonholonomic Systems*. American Mathematical Society.
- Stépán, G. (1991). Chaotic motion of wheels. *Vehicle System Dynamics*, 20:341–351.